Md. (to be published).
[28]J. G. Daunt, in *Progress in Low Temperature Physics*, edited by C. J. Gorter (North-Holland, Amsterdam, 1955).

PHYSICAL REVIEW B VOLUME 2, NUMBER 2 15 JULY 1970

Study of the Interaction of Light with Rough Metal Surfaces. I. Experiment*

D. Beaglehole and O. Hunderi
Department of Physics and Astronomy, University of Maryland, College Park, Maryland 20742
(Received 23 September 1969)

This paper describes measurements of the reflectivity, scattering, and transmission of light by metals with rough surfaces. For surfaces whose roughness is very short ranged, the ratio of rough-surface reflectivity to smooth-surface reflectivity varies exponentially as λ^{-2} both above the plasmon frequency and in regions where $\epsilon_2 \gg |\epsilon_1|$. In the latter regions for these rough surfaces, the scattered intensity follows a λ^{-4} wavelength variation. For surfaces which are more wavy, the reflectivity and scattered light vary less rapidly with wavelength. Well below the plasmon frequency, additional fields not present on smooth surfaces, but coming from induced extra currents and dipoles on rough surfaces, add coherently to the specular beam, with a resonant wavelength variation. Near the plasmon frequency there is extra absorption. We have studied the angular variation of the scattered light, and have observed additional incoherent light associated with these extra dipoles and currents. We compare the experimental results with the scalar scattering theory and make some general comments about the properties of surface dipoles and currents.

I. INTRODUCTION

Light reflected from a smooth homogeneous surface is found only in the specular beam, and its intensity, given by Fresnel's equations, depends upon the polarization of the incident light, the angle of incidence, and the dielectric properties of the bulk medium. When light is reflected from rough surfaces, two new phenomena occur. Firstly, the condition of specularity is relaxed and scattered light is found away from the specular beam, with a reduction in the specular intensity. Fresnel's equations are no longer valid. Secondly, additional currents may be excited, and dipoles induced across pits and bumps on the surface. These can give rise to additional fields which mix with the specular and scattered intensities.

Early theories of the reflection of light from rough surfaces have neglected the effects of additional currents and dipoles. The best-known theory is the "scalar scattering" theory.[1] This considers just the phase modulation of the incident and outgoing light by the height variations along the surface. The specular and scattered light are found by summing the radiation from Huygens wavelets on the surface. The radiation distribution thus depends upon the phase of the wavelets – determined by the phase of the incident field when it reaches a point of the surface – and upon their correlation over the surface. If the height variation is assumed to be normally distributed about its mean with an rms deviation σ, the scalar scattering theory predicts the ratio of the specular reflectivity of a rough surface to that of a smooth surface to vary as $R_r/R_s = e^{-(4\pi\sigma/\lambda)^2}$, and the theory similarly makes predictions about the angular distribution of the scattered light. The scalar scattering theory is energy conserving – all the light lost from the specular beam should appear in the scattered distribution. However, the approximations of the development in Ref. 1 are such that this is only so if the typical distance for variation along the surface a is of the order or greater than λ.

The scalar scattering theory is a simple approach to the interaction of light with rough metal surfaces. It neglects the vector nature of the radiation field and it neglects the distortion of the incident and outgoing fields near the local surface.

A new approach is that of Twersky[2] and Berreman.[3] These authors have considered models representing rough surfaces, models in which it is possible to solve exactly for the electromagnetic fields. The models have consisted of randomly distributed hemispherical bosses, pits, and closely associated shapes on otherwise smooth surfaces. These calculations have been made in

the opposite limit to the scalar scattering theory, namely, when the dimensions of the shapes are much smaller than the light wavelength. Twersky has calculated the scattering from bosses on a perfect conductor. He finds this to vary as λ^{-4}, typical of Rayleigh dipole scattering. Berreman has calculated the first-order coherent contribution to the specular reflectivity for surfaces of any conductivity. He has found that this is especially large at frequencies for which the induced dipoles resonate.

This approach of Twersky and Berreman explicitly takes into account extra dipole fields, but not fields due to currents. That extra currents might be induced on periodically rough (grating) surfaces was first suggested by Fano,[4] and Stern[5] pointed out that randomly rough surfaces would act in a similar fashion. Surface currents, now called surface plasmons, with their associated evanescent electromagnetic fields can exist even on smooth surfaces, but since their wave vector for propagation along the surface is greater than that for a plane-wave light beam, they are not normally excited. Fano pointed out that phase modulation of the incident light by surface waviness can produce a matching of these two wave vectors, and lead to surface-wave excitation.

Dipoles induced across hemispherical and other allied shapes resonate at frequencies such that ϵ_1 is in the range $-\frac{1}{4}$ to -4. Surface plasmons can only exist in regions where ϵ_1 is less than -1. Since metals have a dielectric constant varying with frequency ω typically as $\epsilon_1 = 1 - (\omega_p^2/\omega^2)$($\omega_p$ is the bulk plasmon frequency), the dipole and current effects will be confined to a region where $\omega < \omega_p$ ($\epsilon < 0$) which we will call the metallic region. The region $\omega > \omega_p$ ($\epsilon > 0$) we will call the dielectric region.

Experimentally, there has been little study of either scattering or dipole and current effects on the light reflected from rough metal surfaces. Bennett and Porteus[6] report that scattering from quite smooth surfaces follows the scalar theory's variation at long wavelengths, and, assuming this to be true for rough surfaces, they have used the ratio R_r/R_s in other experiments to find values for σ. Also, a strong decrease in the reflectivity of rough silver surfaces at wavelengths below ω_p has recently been observed by Schnatterly,[7] by Dobberstein *et al.*,[7] and by Stanford *et al.*[7] This has been assumed to indicate extra *absorption* due to surface current excitation. The experiments we report here question both these two assumptions.

We have measured not only R_r/R_s but also the distribution and intensity of the scattered light. This has been done in both the metallic region and the dielectric region. Various metals have been studied, some free-electronlike with $\epsilon_2 \ll |\epsilon_1|$, and others with strong interband absorption where $\epsilon_2 \gg |\epsilon_1|$ – we will call these damped metals. We have compared surfaces of long- and short-wavelength roughness. We have not been able to measure the scattering of the free-electron metals in the dielectric region (though we have measured R_r/R_s), since our scattering equipment does not function in the vacuum ultraviolet.

Our observations are the following. In the dielectric region we find that the scattered light and the specular reflectance have wavelength variations which depend upon the nature of the surface roughness. For short-scale roughness ($a \ll \lambda$) on noble metals the scattered light varies as λ^{-4}, typical of the dipole scattering, while R_r/R_s for these and indeed all metals varies exponentially as λ^{-2}. For wavy surfaces of the noble metals both R_r/R_s and the scattering vary approximately exponentially as λ^{-1}. The angular distribution of the scattered light depends upon the polarization of the incident light.

In the metallic region we show that the changes in reflectance are due to two effects: coherent addition of extra fields at long wavelengths and additional absorption in the resonance region. Underlying the scattered light, we have observed incoherent light associated with the extra fields. In regions where ϵ_2 becomes much larger than $|\epsilon_1|$, strong damping of the extra fields occurs.

Brief reports on sections of this work have already been published.[8] We present full details here and in the following paper, and attempt to provide a unified picture.

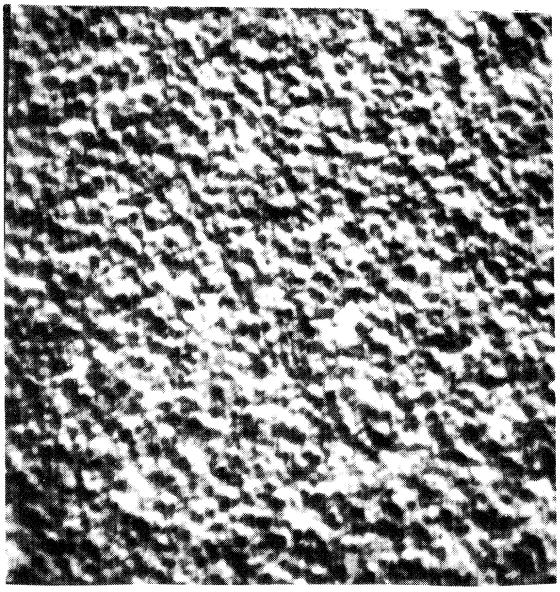

FIG. 1. Electron micrograph of a rough silver surface. Scale: 1 cm = 6500 Å.

FIG. 2. Electron micrograph of a wavy silver surface. Scale: 1 cm = 6500 Å.

II. MEASUREMENTS

In this section, we present the experimental measurements, leaving the discussion to Sec. III. The rough surfaces have been prepared by two methods. We first used the technique of Bennett *et al.*[9] to produce surfaces of very short-wavelength roughness. The method was to evaporate a thin layer of CaF_2 onto a substrate, and then to overcoat with a layer of the desired metal. CaF_2 forms small sharp crystallites, producing surfaces with steep hills and valleys. The distance between hills was roughly 500 Å, while the average height variation of the metal surface could be changed by varying either the amount of CaF_2 deposited or the thickness of the metal layer. An electron micrograph of a typical surface produced in this fashion is shown in Fig. 1.

A second method was used to produce surfaces of indium and silver with a longer wavelength variation. The technique was to anneal the samples until their crystallites grew to several thousand Å in diameter. Migration of atoms away from the crystallite boundaries resulted in samples with waviness of the crystallite dimension. Figure 2 shows an electron micrograph of this type of surface.

Except for those samples used in the transmission measurements, the metal films were all thicker than 1000 Å, and totally opaque. Where we have compared rough samples with smooth samples, the substrates for the latter were specially polished, and both the smooth and rough

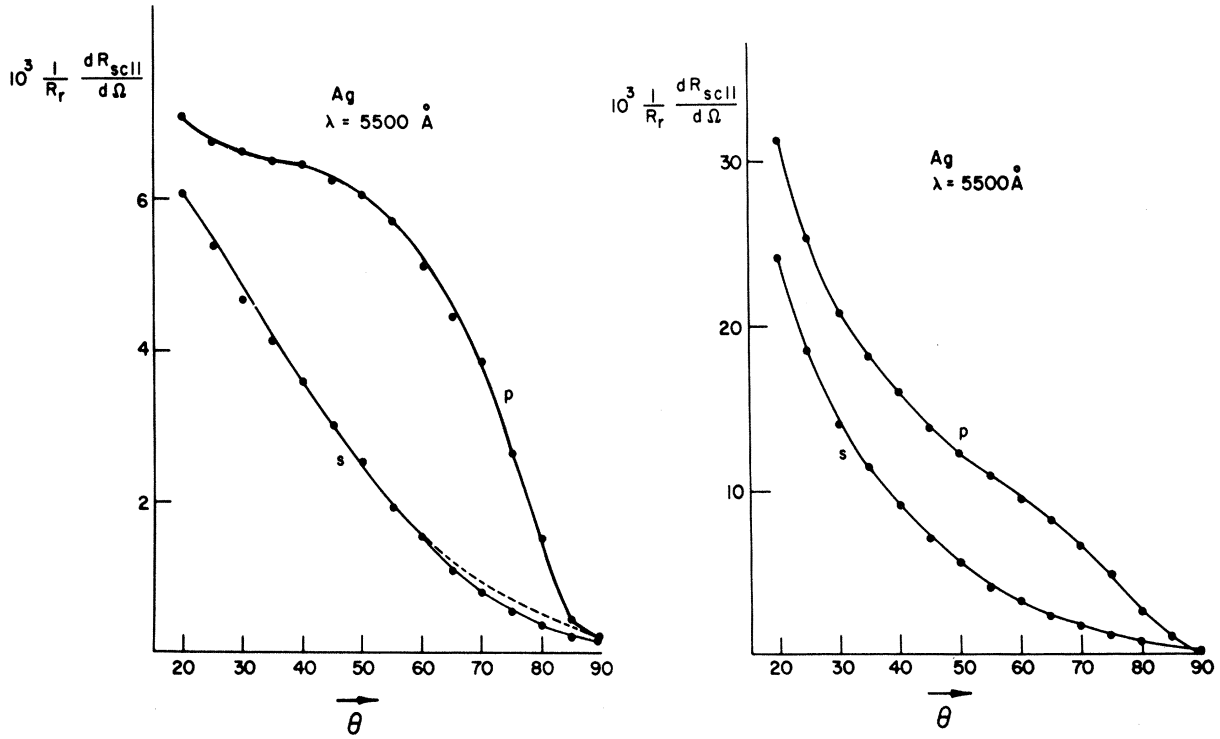

FIG. 3. Angular distribution of the fractional scattered intensity measured with analyzer and polarizer parallel; left, for a rough silver surface; right, for a wavy silver surface. The dotted line shows a fit to the scalar theory.

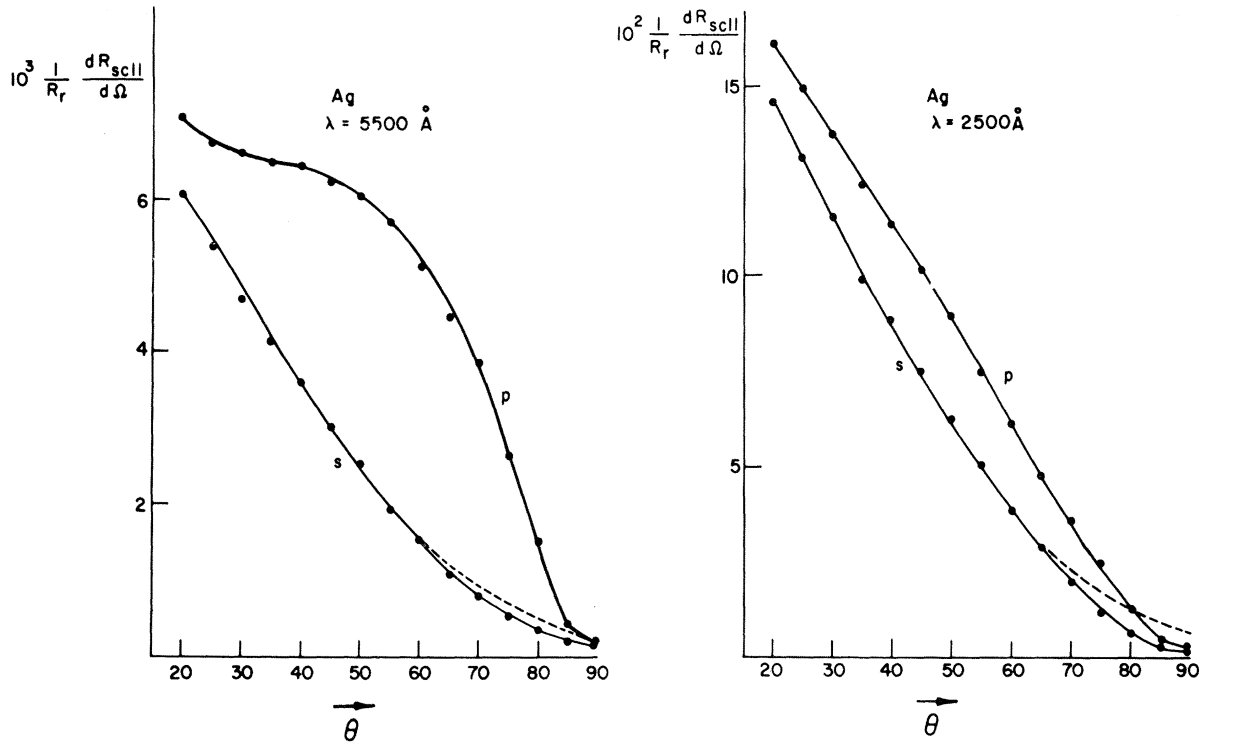

FIG. 4. Comparison of the angular distribution of the fractional scattered intensity in the metallic and dielectric regions for a rough silver surface. The dotted line shows a fit to the scalar theory with $a = 1300$ Å at 5500 Å, and 550 Å at 2500 Å.

samples were prepared during the same evaporation.

A. Scattering of Light

A parallel beam of light was normally incident onto the sample, and the radiation scattered measured as a function of the angle θ from the normal. The detector had a circular aperture, subtending a solid angle of 0.007 sr.[2] The incident light was polarized in either the s or p direction with respect to the observation plane (s-polarized light has its $\vec{E}$ vector perpendicular to the observation plane) and an analyzer could be placed in the outgoing beam.

In Figs. 3 and 4, we show typical examples of the angular variation of the scattered light. R_{sc} is the total scattered intensity divided by the incident intensity. $(1/R_r)dR_{sc}/d\Omega$ is the scattering per unit solid angle relative to the rough-surface reflectivity with no analyzer in the outgoing beam. $(1/R_r)dR_{sc}\,||/d\Omega$ and $(1/R_r)dR_{sc}\perp/d\Omega$ are the scattering per unit solid angle relative to the rough-surface reflectivity with an analyzer oriented, respectively, parallel or perpendicular to the incident polarization. Figure 3 is for silver samples in the metallic region, and compares the scattering of very rough and wavy surfaces. The scattered light falls more rapidly with angle for the latter. In both cases the p-incident light is scattered more strongly than s. We find a knee in the p distribution, rather weak with the wavy samples, while the s falls continually with θ.

A comparison of the scattering in the metallic region with the scattering in the dielectric region indicates those features of Fig. 3 which are particularly associated with the metallic region. This comparison is shown in Fig. 4 for the rough silver surface. p light in both cases is more strongly scattered than s. The knee is absent in the dielectric region. The knee is thus associated with the metallic region, and appears to be due to extra light peaking around $\theta = 60°$.

The additional component is seen more clearly if the analyzer is used in the outgoing beam, orientated perpendicular to the incident polarization. In this way we measure light which has its plane of polarization rotated 90° in the scattering process. In Fig. 5, we show the angular variation of this light for rough and wavy silver samples in the metallic region; in Fig. 6, we compare the dielectric region with the metallic region for the rough silver sample; in Fig. 7 we compare the damped metallic region with the free-electron metallic region for a rough gold sample. When s light is incident, p scattered, a strong anomaly is seen in the free-electron metallic region, but not

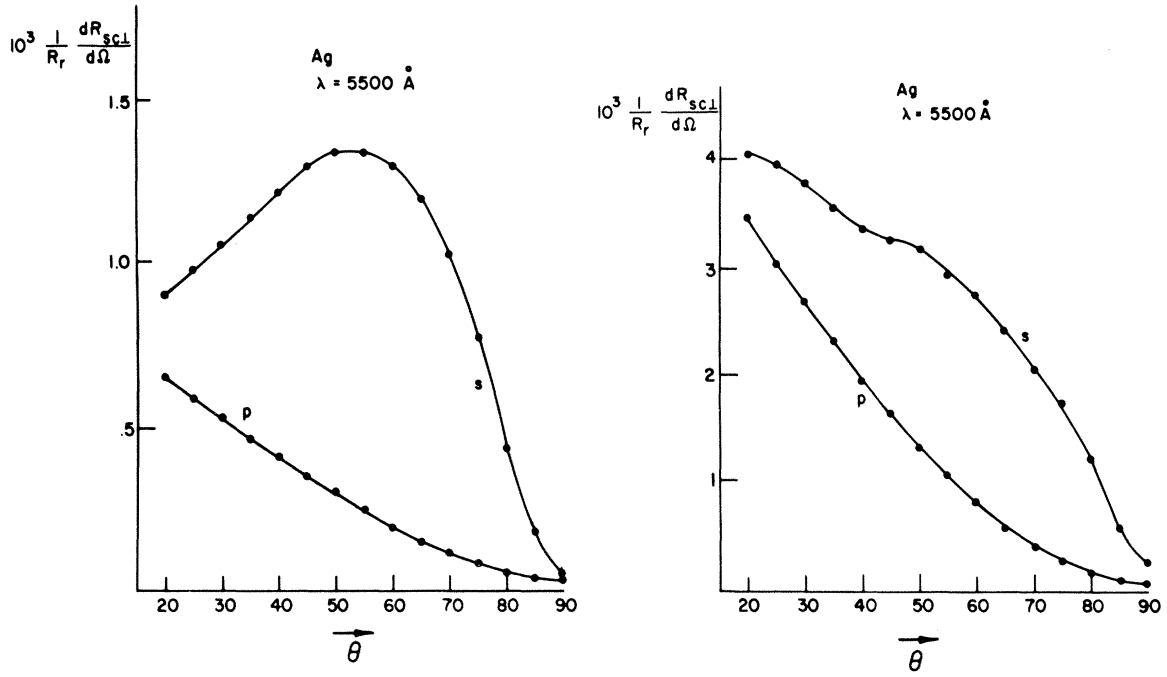

FIG. 5. Angular distribution of the fractional intensity measured with analyzer and polarizer crossed; left, for a rough silver surface; right, for a wavy silver surface.

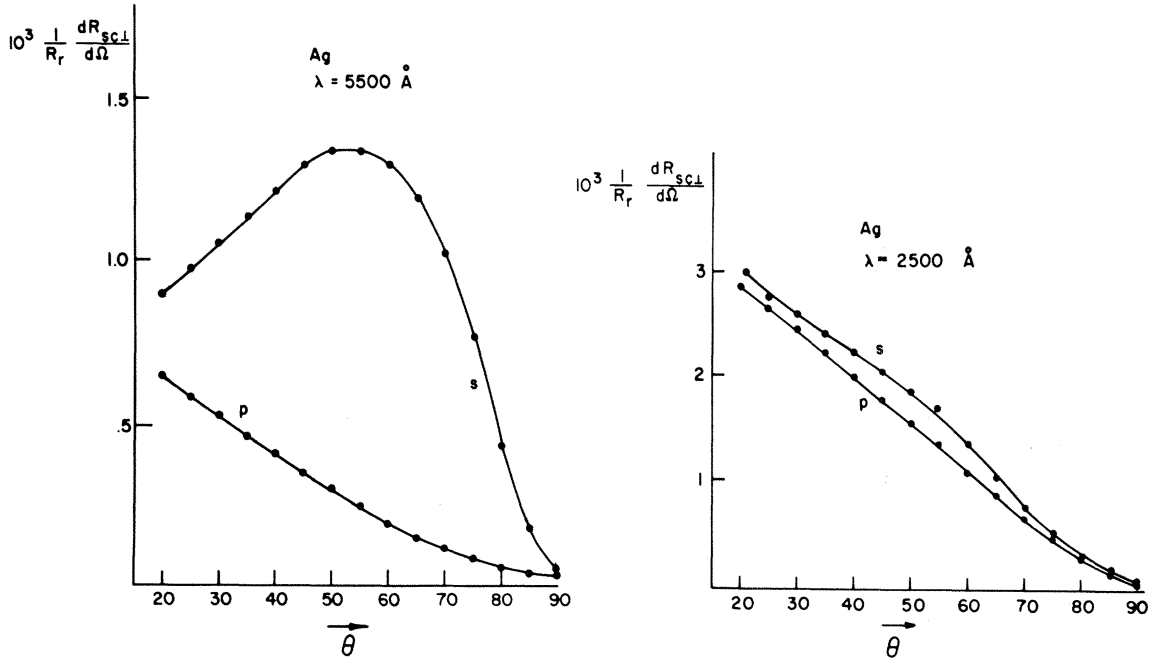

FIG. 6. Angular distribution of the fractional intensity measured with analyzer and polarizer crossed; comparison for a rough silver surface with the metallic region, left; with the dielectric region, right.

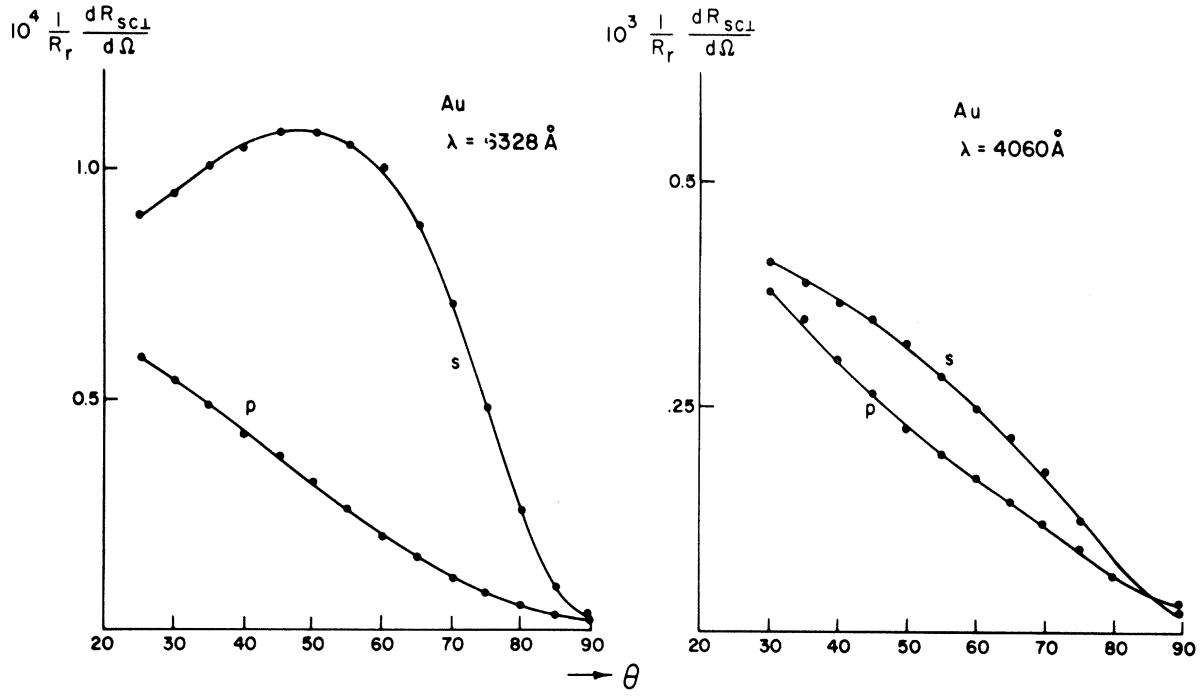

FIG. 7. Angular distribution of the fractional intensity measured with analyzer and polarizer crossed; comparison for a rough gold surface with the metallic region, left; and damped region, right.

in the dielectric region, nor in the damped metallic region. Nor is it observed with p-incident–s-scattered light. The anomalous scattered light is therefore always p polarized.

To study the wavelength variation of the total scattered light, we have averaged the s and p curves of Figs. 3 and 4 at each value of θ, and then integrated over the total scattering hemisphere. Dividing by the incident intensity, we have obtained the total scattered fraction R_{sc}/R_r. We have also estimated the intensity associated with the anomaly in the metallic region. The contribution for s-incident–p-scattered light has been found from Figs. 5 and 7. We have taken the difference between the s and p curves of these figures, and again integrated over the hemisphere. There will also be a contribution from p-incident $-p$-scattered light, producing the knee in Figs. 3 and 4. It is impossible to isolate this component from the background scattered light; however, a simple theory (see the following paper) suggests that this component should be about three times larger than the measured s-incident–p-scattered component. We have therefore used this factor in estimating the total anomalous intensity.

In Fig. 8, we have plotted $R_r/(R_r+R_{sc})$ versus λ^{-2} for rough silver, gold, and copper samples. Recall that the scalar scattering theory predicts $R_r/(R_r+R_{sc})$ to vary as $e^{-(4\pi\sigma/\lambda)^2}$, which would produce straight lines on this plot. The anom-

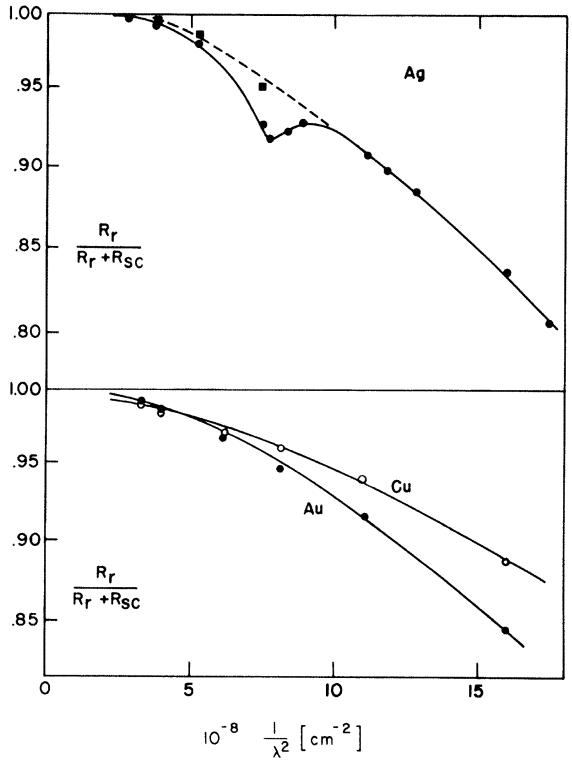

FIG. 8. $R_r/(R_r+R_{sc})$ versus λ^{-2} for silver, gold, and copper with corrections for the observed anomaly. The scalar scattering theory predicts straight lines for the variation on this plot.

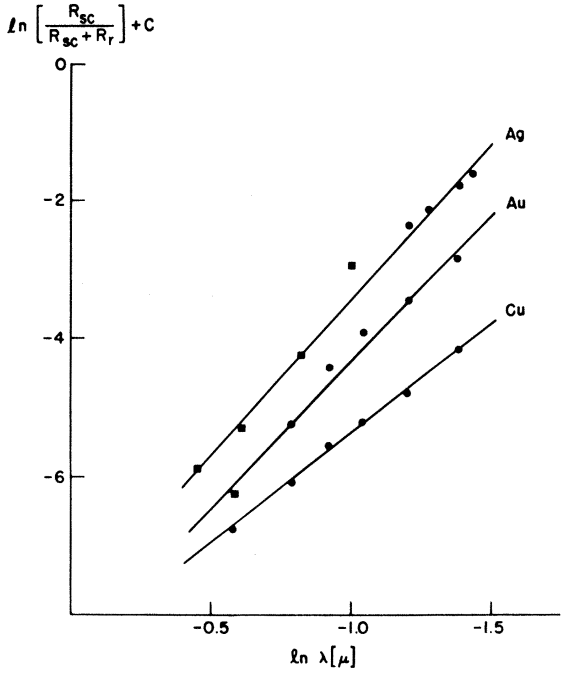

FIG. 9. Data of Fig. 8 plotted on a ln-ln scale. The slope of the lines 4.5 for silver, 4.1 for gold, and 3.2 for copper.

alously large scattering for the silver sample in its metallic region is again clearly apparent. We obtain the dotted curve when the estimated anomalous intensity is subtracted off. The data points for copper and gold samples lie in their dielectric region.

We do not find straight lines on this graph. Clearly the scattered radiation even when corrected for the anomaly is not varying exponentially with λ^{-2}.

In Fig. 9, we show the same data plotted as $\ln[R_{sc}/(R_{sc}+R_r)]$ versus $\ln\lambda$. Straight lines are obtained of slope near -4, indicating that $R_{sc}/(R_{sc}+R_r)$ varies as λ^{-4}.

In Fig. 10, we show the wavelength variation of the anomalous radiation for the rough silver sample. It lies entirely in the metallic region, strongly peaked just below the point where the sample's dielectric constant equals -1, shown labeled as λ_{sp}. We return to these data later.

B. Reflection of Light

We have compared the reflectivity of rough samples with smooth samples, measuring $(R_s - R_r)/(R_s + R_r)$ by the comparison method of Beaglehole.[10] The wavelength range was 8000 – 1200 Å.

In Fig. 11, we show the quantity $(R_s - R_r)R_s$ for rough gold, silver, and indium samples; in Fig. 12 for an aluminum sample. On the λ axis we have marked the wavelengths for which $\epsilon_1 = -1$ (λ_{sp}) and $\epsilon_1 = 0$ (λ_p). The dielectric region lies to wavelengths shorter than λ_p, the metallic region to longer wavelengths. ΔR equals $R_s - R_r$.

Despite their different reflectivity, we see that the effects of roughness are remarkably similar in all these metals. Characteristically, there is a steadily increasing $\Delta R/R_s$ throughout the whole range, with an anomalous increase in this quantity (and thus a decrease in R) for wavelengths longer than λ_{sp}. The curve for rough silver is similar to that found by the authors mentioned in Sec. I, although they do not appear to have realized that the anomalous peak is superimposed upon the steadily increasing background.

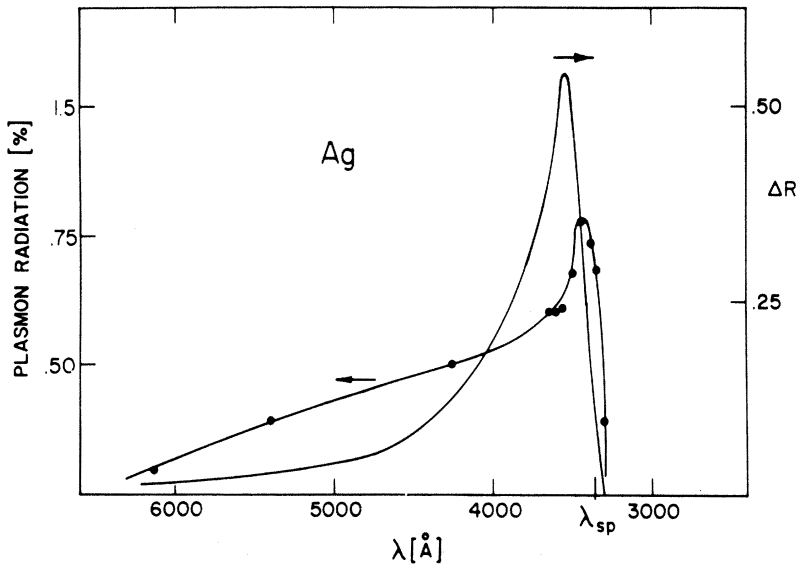

FIG. 10. Total anomalour radiation compared with total decrease in reflectivity for a rough silver surface.

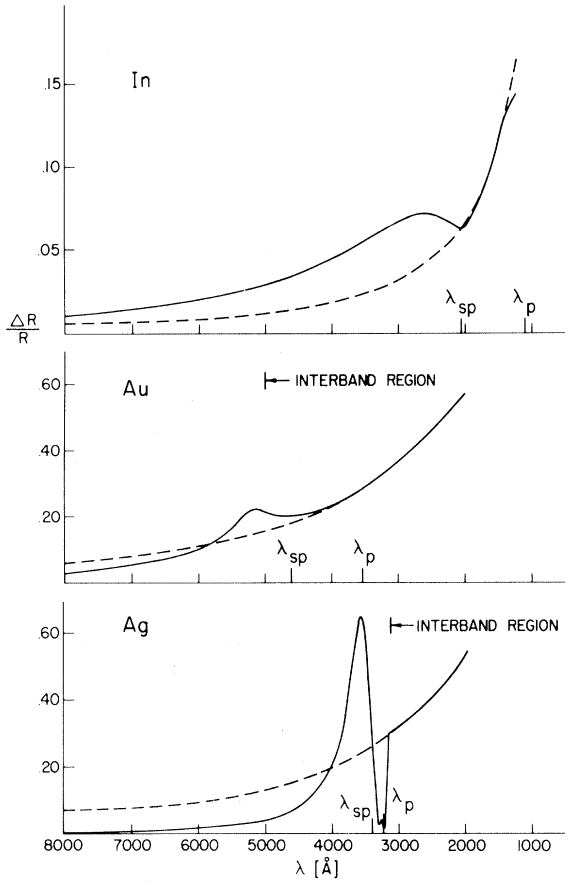

FIG. 11. Fractional decrease in reflectivity plotted versus wavelength for rough indium, gold, and silver surfaces.

λ_{sp} and λ_p are close together for silver. For indium, however, these wavelengths are well separated. The steadily increasing background is seen to continue smoothly through this portion of the metallic region into the dielectric region. In copper and gold, the anomalous peak is well separated from λ_{sp}, occurring at the reflectivity

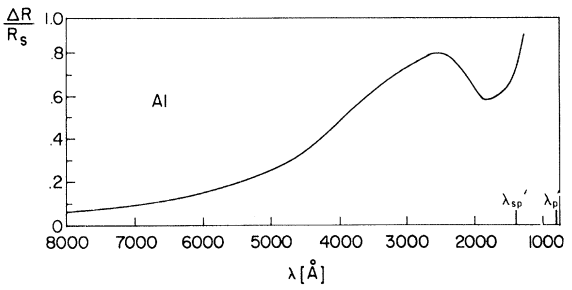

FIG. 12. Fractional decrease in reflectivity plotted versus wavelength for a rough aluminum surface. The sample has a thin MgF overcoating to protect against oxidation and λ_{sp}' has been modified to include this overcoating.

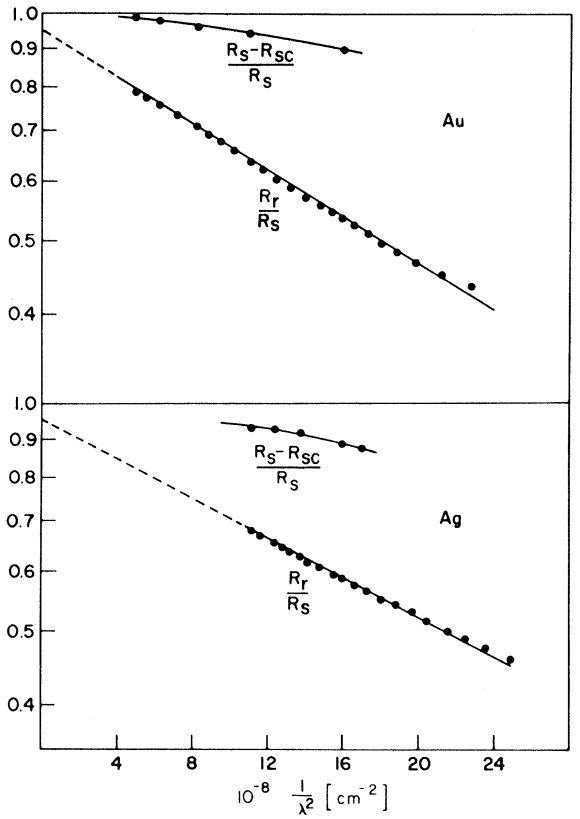

FIG. 13. R_r/R_s and $(R_s - R_{sc})R_s$ versus λ^{-2} for rough silver and gold.

edge, above which interband transitions damp the free-electron properties.

Some of the decrease in the specular reflectivity is due to the scattering of Sec. II A. We have found typically for the rough surfaces that the total scattered intensity is less than $\frac{1}{4}$ of ΔR (Figs. 13 and 14). Most of the background decrease is therefore due to a nonradiative interaction at the surface.

To illustrate the wavelength variation of the rough-surface reflectivity, we have plotted $\ln(R_r/R_s)$ versus λ^{-2} for rough silver and gold samples in Fig. 13, and for indium in Fig. 14. The plots cover the region of wavelengths shorter than λ_{sp} for indium (essentially a free-electron metal), and in the case of the noble metals also the region of strong damping. The data fall on remarkably straight lines, extrapolating close to zero as λ^{-2} tends to zero. Thus, although the scattered light does not vary exponentially with λ^{-2} as we saw in Sec. II A, the ratio R_r/R_s does. This exponential variation is shown by the dashed extrapolated lines at wavelengths longer than λ_{sp} in Fig. 11. Interestingly, the extrapolation crosses the experimental $\Delta R/R_s$ curves of silver

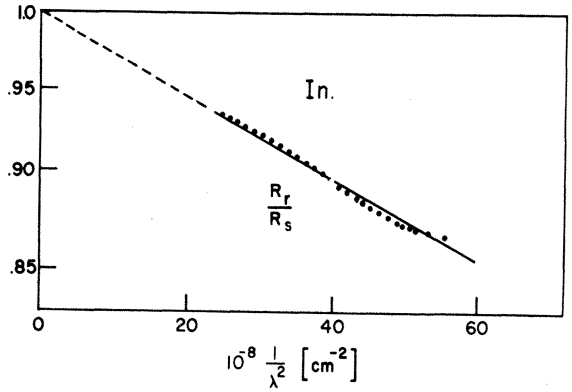

FIG. 14. R_r/R_s versus λ^{-2} for rough indium.

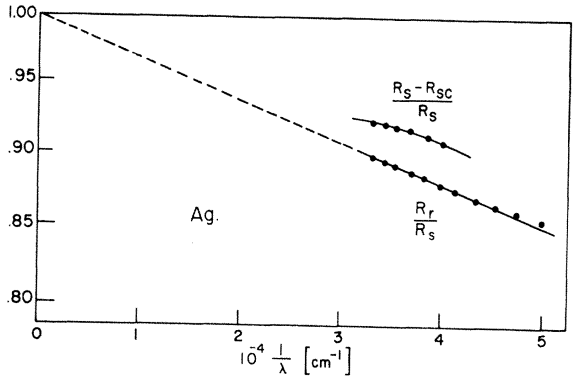

FIG. 16. R_r/R_s and $(R_s - R_{sc})/R_s$ versus λ^{-1} for a wavy silver surface.

and gold, and will do so for the other metals at longer wavelengths. We will return to our interpretation of this effect in Sec. III.

In Fig. 15, we compare smooth and wavy silver samples. The structure near λ_{sp} is much less pronounced with the wavy sample. For wavelengths shorter than λ_p the wavy silver sample has a slower wavelength variation than the rough sample, $\ln(R_r/R_s)$ varying approximately as λ^{-1} (Fig. 16). Again the extrapolated variation to wavelengths longer than λ_p cuts the actual $\Delta R/R_s$ curve. For these wavy samples we have found the scattered light to be reproducibly a little greater than the decrease in reflectance. The error bars are shown in Fig. 15.

C. Transmission

A typical curve comparing the transmission of rough and smooth silver samples is shown in Fig. 17, where we plot $(T_s - T_r)/T_s = \Delta T/T_s$, where T_s is the transmission of a smooth sample and T_r of a rough sample. The samples of this example were 700 Å thick Characteristically, we find more transmission by the rough sample at long wavelengths, then a region of less transmission near λ_{sp}, and again less transmission for wavelengths much shorter than λ_p. The zero in ΔT falls close to the "zero" in ΔR (Fig. 11). For completeness T_r is also shown in this figure.

III. DISCUSSION

We consider first the dielectric region where we have found the simplest behavior. To summarize, with rough noble-metal surfaces ($\epsilon_2 \gg \epsilon_1$) we have observed a λ^{-4} variation of the scattered light, its intensity being much smaller than the decrease in specular reflectance: The specular reflectance itself varied as $R_r/R_s = \exp(-A/\lambda^2)$. This specular reflectance variation was found also with free-electron metals. With wavy surfaces the wavelength variations of both the scattered light and R_r/R_s were less rapid.

The most important of these is the observation

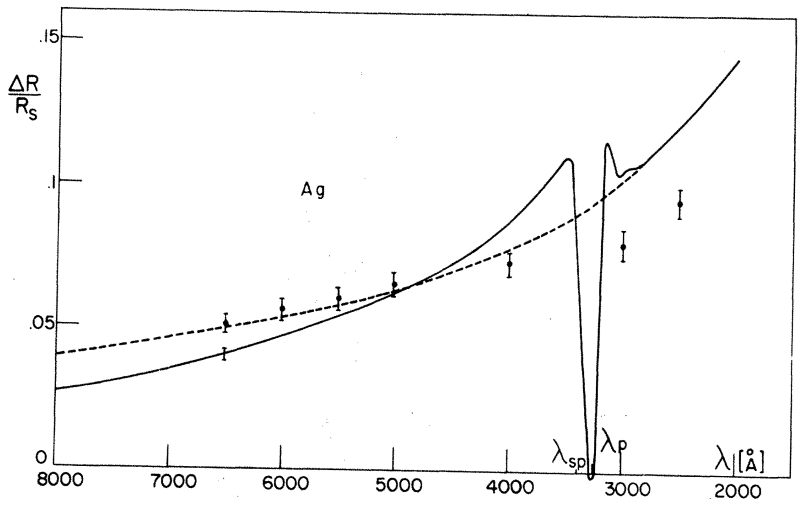

FIG. 15. Fractional decrease in reflectivity and the total fractional scattering of a wavy silver surface.

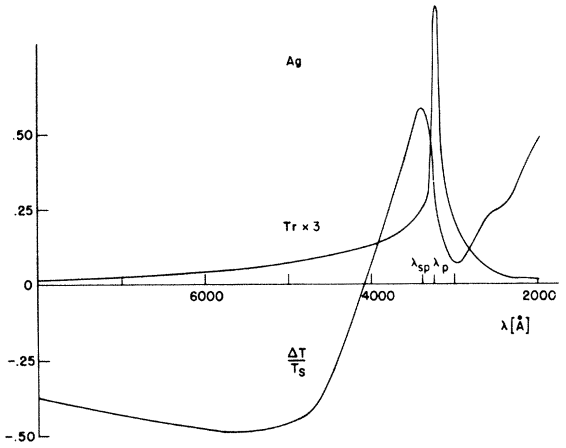

FIG. 17. Fractional change in the transmission $\Delta T/T_s$ and the transmission T_r of a 700-Å rough-silver film plotted versus wavelength.

of the nonradiative decrease in reflectance. This is a surface absorption effect. We have found it to be *absorption* since otherwise we would have observed an extra transmittance in this region, and we have found it to be a *surface* effect, since extra bulk absorption in this region would raise the sample's reflectivity.[11]

This nonradiative component indicates immediately limitations to the theories of scattering which are energy conserving, and it leads to inconsistency in their application to the data. Consider the scalar scattering theory which is energy conserving. The theory predicts $R_r/R_s = \exp[-(4\pi\sigma/\lambda)^2]$ which fits our experimental data. It predicts the scattered light (for normally incident light) to vary with angle and wavelength as

$$R_{sc} \propto \frac{a^2\sigma^2}{\lambda^4}\ (\cos\theta+1)^4 \exp\left(-\frac{\pi^2 a^2}{\lambda^2}\sin^2\theta\right).$$

In Fig. 3, we show that this expression does reproduce the angular variation of the s-incident scattered light but not the p-incident scattered light if $\pi a/\lambda \ll 1$, and in this limit the expression predicts the observed λ^{-4} wavelength variation. Thus, applying these two expressions one might expect to evaluate both σ and a. However, this is an uncertain procedure, because the expressions are only valid in the opposite limit $\pi a/\lambda \gg 1$. The decrease in the reflectance in theory should equal the scattered light. Experimentally this inconsistency shows up when fitting the second expression to the scattered light, for we find that the parameter a has to be wavelength dependent. In fact we will argue below that the λ^{-4} variation is only characteristic of metals where $\epsilon_2 \gg |\epsilon_1|$ and not the variation one would find for free-electron metals. The agreement of the scalar-scattering-theory predictions with experiment appears to be fortuitous. While the expression for R_r/R_s does very well in the region where it is not applicable, it does not do well in the region where it is. We have found the wavy surface to show a less rapid wavelength variation, although this may be the result of a non-normally distributed roughness on these surfaces.

The microscopic approach of Twersky and Berreman appears most fruitful for an understanding of the origin of the wavelength and angular variation of the scattered light. As we have mentioned in Sec. I, these authors considered the properties of a random array of small hemispherical bumps and pits and other shapes placed on smooth surfaces. Twersky has calculated the scattering for perfect conductors, which he finds varies as λ^{-4} for hemispheres and as λ^{-3} for hemicylinders. Berreman has calculated the reduction in the specular reflectivity due to absorption losses by the induced dipoles for surfaces with realistic values of ϵ_1 and ϵ_2.

The properties of isolated spheres are quite similar to those of hemispheres on a metal surface, as we will describe in the following paper, so we review them briefly for they provide a good deal of insight into the scattering and absorption processes. The theory for scattering and absorption by isolated spheres has been solved exactly by Mie[12] for all wavelengths of light and arbitrary values of the sphere diameter and dielectric constant. The solution is discussed in detail by van de Hulst.[13] The results are written in terms of the scattering and absorption cross sections Q_{sca} and Q_{abs}, respectively, defined by

$$\frac{I_{sca}}{I_0} = \pi a^2 Q_{sca}, \quad \frac{I_{abs}}{I_0} = \pi a^2 Q_{abs},$$

where I_{sca} is the total scattered intensity, and I_{abs} the total absorbed intensity. I_0 is the incident intensity.

For small spheres such that $x = 2\pi a/\lambda \ll 1$, where a is the radius of the spheres, Mie's solution takes a simple form. The effective polarizability of a sphere is $(3/4\pi)/[(\epsilon-1)/(\epsilon+2)]$. The scattering cross section is proportional to $x^4\,|\,(\epsilon-1)/(\epsilon+2)\,|^2$ while the absorption cross section is proportional to $x\,\mathrm{Im}[(\epsilon-1)/(\epsilon+2)]$. In metals where ϵ takes negative values, both the scattering and absorption show resonant behavior at $\epsilon = -2$. Twersky's calculation corresponds to an evaluation of Q_{sca} in the region $|\epsilon_1| \gg 1$, $\epsilon_2 = 0$. In this region $[(\epsilon-1)/(\epsilon+2)]^2$ is independent of wavelength, and an x^4 wavelength variation of the scattering is obtained. Berreman's calculation corresponds to evaluation of Q_{abs} only, the specular reflectivity being reduced

TABLE I. Wavelength variation of the scattering and absorption of small metal spheres. For $x \ll 1$,

$$Q_{sca} = \frac{8}{3}x^4 \frac{(\epsilon_1 - 1)^2 + \epsilon_2^2}{(\epsilon_1 + 2)^2 + \epsilon_2^2}, \quad Q_{abs} = 12x \frac{\epsilon_2}{(\epsilon_1 + 2)^2 + \epsilon_2^2}.$$

For a free-electron metal $\omega\tau \gg 1$, $\epsilon_1 = 1 - \omega_p^2/\omega^2$, $\epsilon_2 = \omega_p^2/\omega^3\tau$.

Region	Q	Expression	Wavelength variation	Experimentally observed for rough surfaces
(a) Free-electron metal				
$\lambda \gg \lambda_p$	Q_{sca}	$\frac{8}{3}x^4$	λ^{-4}	λ^{-4}
	Q_{abs}	$12x\,\epsilon_2/\epsilon_1^2$	λ^{-2}	
$\lambda < \lambda_p$	Q_{sca}	$\frac{8}{27}x^4(\epsilon_1 - 1)^2$	const	
	Q_{abs}	$\frac{12}{9}x\epsilon_2$	λ^{-2}	
(b) Damped metal				
$\epsilon_2 \gg \lvert\epsilon_1\rvert$	Q_{sca}	$\frac{8}{3}x^4$	λ^{-4}	λ^{-4}
	Q_{abs}	$12x/\epsilon_2$		

by light absorbed.

It is interesting to estimate the wavelength variation of the scattering and absorption of small spheres in the dielectric and metallic regions. These are listed in Table I. We find the scattering in the damped region again follows a λ^{-4} variation, while free-electron metals in the dielectric region follow a λ^{-2} variation. The former corresponds very well with our experimental observations on the noble metals.

It is also interesting to compare the relative magnitudes of Q_{abs} and Q_{sca} for small spheres. We have calculated these using values of ϵ_1 and ϵ_2 for bulk samples keeping terms up to a_5 and b_5 in Mie's solution.[13] We show their wavelength variation in Fig. 18 for silver, copper, and gold spheres, 400 Å in radius. In the damped dielectric region we see that the ratio is roughly constant, of the order of 3. The ratio Q_{abs}/Q_{sca} depends very sensitively on a, varying approximately as a^{-3}. The value of 400 Å was chosen since it led approximately to the experimentally observed ratio of nonradiative decrease in reflectance to scattered light. This value of a is surprisingly close to the value found using the electron micrograph. Q_{abs} is less than Q_{sca} at longer wavelengths. For copper and gold spheres $\epsilon_1 = -2$ in the interband region. The resonance is strongly damped, reaching the peak below the absorption edge. Figure 19 shows the variation of Q_{abs} and Q_{sca} for a free-electron metal whose parameters have been chosen to be approximately those of aluminum, and for a transparent dielectric (Q_{abs} in this case is equal to zero).

If we make a correspondance between spheres and rough metal surfaces – this will be discussed further in the following paper – these results suggest that the decrease in reflectance in the vicinity of the resonance region is mainly due to absorption losses, while there is a resonance in the scattering. In the interband region absorption losses are clearly the cause for the nonradiative decrease. At longer wavelengths where Q_{abs}/Q_{sca} is less than unity the additional coherent radiated fields will be important in determining the changes in specular reflectance.

These predictions agree well with our experimental results. Looking back at Figs. 11 and 17,

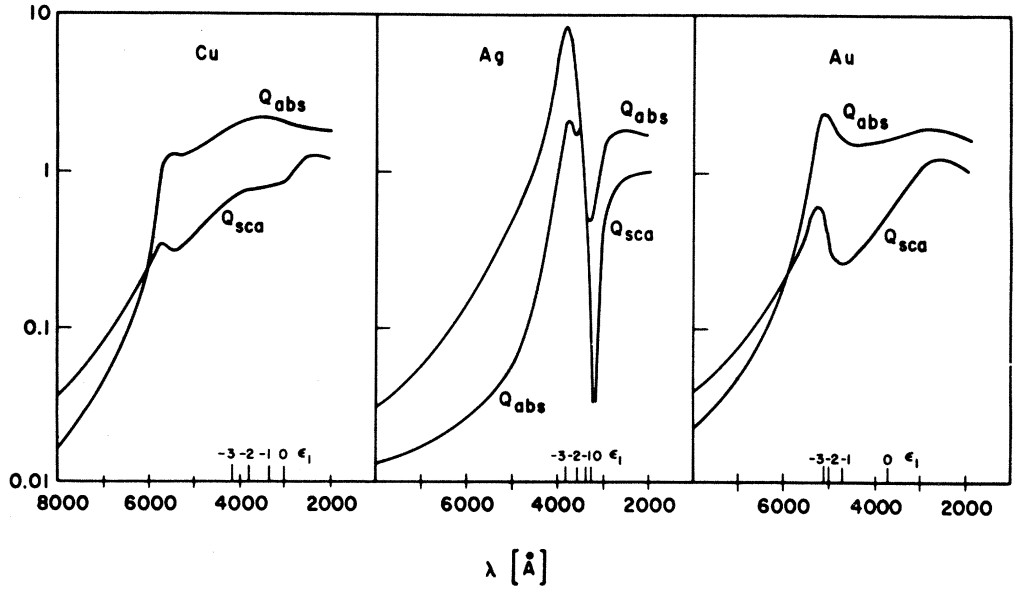

FIG. 18. Absorption cross section Q_{abs} and scattering cross section Q_{sca} for isolated silver, copper, and gold spheres of 400-Å radius.

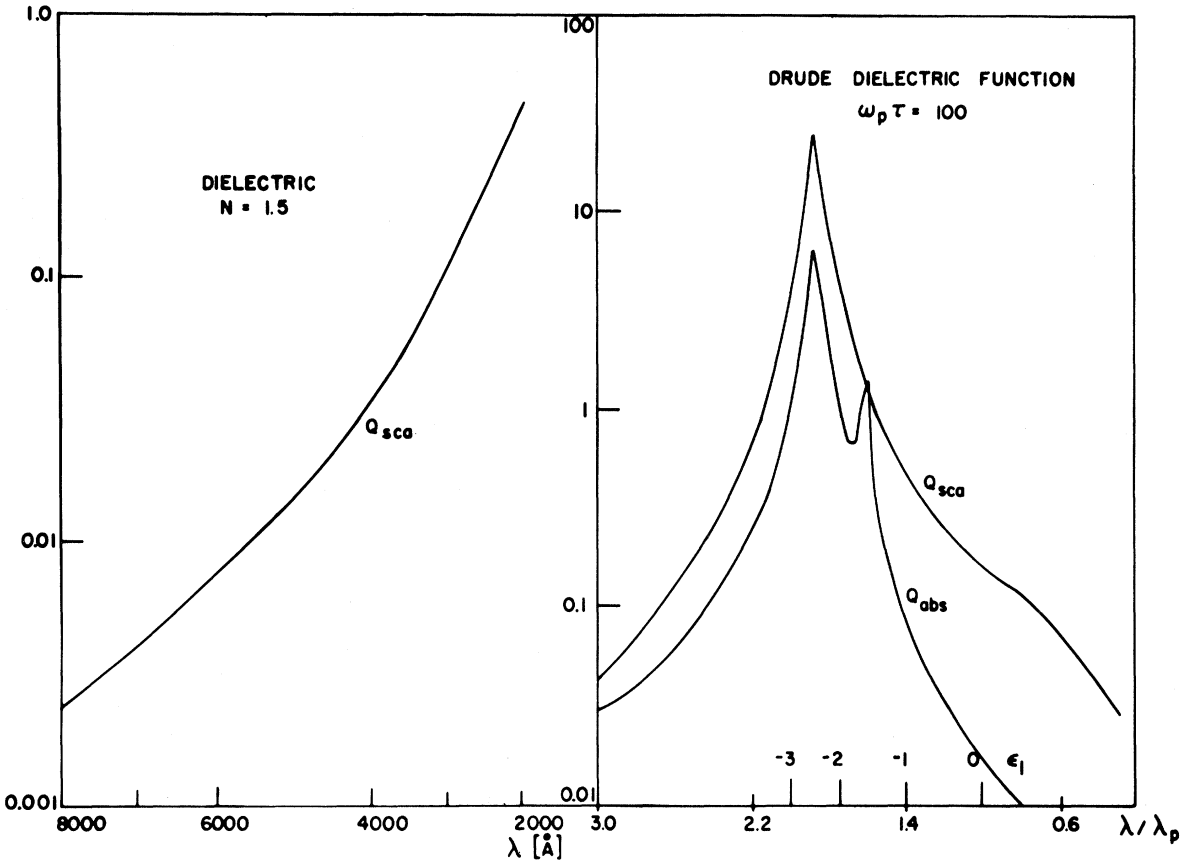

FIG. 19. Absorption cross section and scattering cross section for a Drude free-electron dielectric constant and for a transparent dielectric constant.

which show $\Delta R/R_s$ and $\Delta T/T_s$, we see the following. Well below the resonance region, where a decrease in reflectance occurs, there is an increase in transmittance; thus there is little extra absorption. In the vicinity of the resonance where $\Delta R/R$ is greatest we find less transmittance. Here we have extra absorption. The crossover point where $\Delta T = 0$ occurs at 4100 Å, which is close to the point where spheres show Q_{abs}/Q_{sca} equal to unity.

Additional proof that at long wavelengths additional coherent fields *increase* a metal's reflectivity over the decrease which would be expected if dipoles and currents were neglected is found in the results for the wavy silver surface, shown in Fig. 15. We see that for wavy surfaces the nonradiative term is much smaller than for rough surfaces, being only about $\frac{1}{4}$ of $\Delta R/R_s$ in the dielectric region for the latter. At long wavelengths the scattered light component is actually *greater* than $\Delta R/R_s$, thus indicating that the specular reflectance is higher than otherwise expected.

It is also to be expected that R_r/R_s would vary less rapidly for wavy surfaces than for rough surfaces as we found, since the coefficients of x in the scattering and absorption equations are smaller for cylinders than for spheres.

The experimental $\Delta R/R_s$ curves for copper and gold show the maximum in ΔR falling well below the resonant point in ϵ, the maximum occurring at the interband absorption edge. This is the point at which ϵ_2 increases rapidly to become greater than $|\epsilon_1|$, damping the resonance. Even on the best of samples grain boundaries provide a source for dipole effects, and we suggest that these, along with the surface currents described below, are the cause for the surprisingly rounded reflectivity edges which have always been found with these metals.

An alternative approach to the additional fields and absorption which occur with rough surfaces is that initiated by Stern,[5] which considers the excitation of surface plasmons. These are not excited on smooth surfaces, since the plasmon wave vector along the surface is greater than ω/c, but they may be excited when the surface is rough. For a review of surface plasmon properties see Steinmann.[14] In this approach one

considers the roughness-induced scattering of the incident light into surface plasmon modes, and subsequent decay of the surface plasmons by absorption or reradiation through further scattering. The model appears especially suited to the case of metal gratings[15] and to cases where the scattering of surface plasmons is weak.[16] We will show in the following paper that the model predicts the angular variation of the s- and p-scattered light and the anomalous light quite well. In this approach, however, it is necessary to make assumptions about the strength of the coupling between surface plasmon and roughness, and it is difficult to incorporate absorption consistently into the model. The microscopic approach we have outlined above appears more intuitive, especially for the case of rough surfaces with short-wavelength variations.

---

*Research supported by the Advanced Research Projects Agency.

[1]H. Davis, Proc. Inst. Elec. (London) Engrs. 101, 209 (1954); P. Bechman and A. Spizzichino, *The Scattering of Electromagnetic Waves from Rough Surfaces* (Pergamon, New York, 1963).

[2]V. Twersky, IRE Trans. Antennas Propagation AP-5, 81 (1957).

[3]D. W. Berreman, Phys. Rev. 163, 855 (1967).

[4]U. Fano, J. Opt. Soc. Am. 31, 213 (1941).

[5]E. A. Stern, in *Optical Properties and Electronic Structure of Metals and Alloys*, edited by F. Abeles (North-Holland, Amsterdam, 1966).

[6]H. E. Bennett and J. O. Porteus, J. Opt. Soc. Am. 51, 123 (1969).

[7]P. Dobberstein *et al.*, in Proceedings of the Second International Vacuum Ultraviolet Conference, Gatlinsburg, Tennessee, 1968 (unpublished); J. L. Stanford *et al.*, *ibid.*; S. E. Schnatterly, *ibid.*; also, S. N. Jasperson and S. E. Schnatterly, Phys. Rev. 188, 759 (1969).

[8]O. Hunderi and D. Beaglehole, Phys. Letters 29A, 335 (1969); O. Hunderi and D. Beaglehole, Optics Commun. 1, 101 (1969).

[9]H. E. Bennett, J. M. Bennett, E. J. Ashley, and R. J. Motyka, Phys. Rev. 165, 755 (1968).

[10]D. Beaglehole, Appl. Opt. 7, 2218 (1968).

[11]$dR/d\epsilon_2 > 0$ if $\epsilon_2 > (1 - 2\epsilon_1 + 3\epsilon_1^2)^{1/2}$, which is true for all the noble metals in their interband region.

[12]G. Mie, Ann. Phys. (N. Y.) 25, 377 (1908).

[13]H. C. van de Hulst, *Light Scattering by Small Particles* (Wiley, New York, 1957).

[14]W. Steinmann, Phys. Status Solidi 28, 437 (1968).

[15]Y. Y. Teng and E. A. Stern, Phys. Rev. Letters 19, 511 (1967); R. H. Ritchie, E. T. Arakawa, J. J. Cowan, and R. N. Hamm, *ibid.* 21, 1530 (1968).

[16]R. E. Wilems and R. H. Ritchie, Phys. Rev. Letters 19, 1325 (1967); P. A. Fedders, Phys. Rev. 165, 580 (1968).

PHYSICAL REVIEW B VOLUME 2, NUMBER 2 15 JULY 1970

Study of the Interaction of Light with Rough Metal Surfaces. II. Theory*

O. Hunderi and D. Beaglehole

Department of Physics and Astronomy, University of Maryland, College Park, Maryland 20742

(Received 23 September 1969)

In the preceding paper we described the measurements of the scattering, reflectivity, and transmission of light by metals whose surfaces were rough on a microscopic scale. In this paper we develop further the two theoretical approaches outlined in that paper. The first approach considers the radiation from surface currents modulated by the surface roughness. The second approach considers a model surface for which the reflection properties can be solved exactly, the model consisting of metal spheres located above a smooth metal surface. The two approaches demonstrate all the physical phenomena reported in the preceding experimental paper.

I. INTRODUCTION

The optical properties of the various rough surfaces we investigated in the preceding paper were surprisingly similar, depending mainly upon whether we were in a metallic region, a dielectric region, or a damped metallic region. However, none of the theories referred to in that paper gave a satisfactory description of their properties.

In this paper, we develop two different approaches to the problem of absorption and scattering by rough metal surfaces. The first approach considers the radiation from surface currents induced by the incident light. The surface currents are taken to be of two parts: the usual polarization currents of a smooth surface now modulated by the roughness,

FIG. 1. Electron micrograph of a rough silver surface. Scale: 1 cm = 6500 Å.

FIG. 2. Electron micrograph of a wavy silver surface. Scale: 1 cm = 6500 Å.